

# Determination of residual stresses in three-layer alumina composites using an indentation technique

JIHONG SHE

*Shanghai Institute of Ceramics, Chinese Academy of Sciences, 1295 Ding-Xi Road, Shanghai 200050, People's Republic of China*

S. SCHEPPOKAT, R. JANSSEN, N. CLAUSSEN

*Advanced Ceramics Group, Technische Universität Hamburg-Harburg, 21073 Hamburg, Germany*

The distribution of residual stresses in three-layer reaction bonded alumina (RBAO) composites with 17.5 vol % zirconia in the inner layer and 40 vol % mullite in the outer layers was determined by an indentation technique. It could be shown that the outer layers are subject to a residual compressive stress while the inner layer is under a tensile stress. With increasing outer layer thickness, the residual compressive stress decreases, and the residual tensile stress increases. Compressive stresses up to 550 MPa were measured in this study. It was found that the residual stresses are not uniform throughout the layers. The magnitude of the stresses decreases with increasing distance from the interfaces. This is attributed to creep during cooling from the sintering temperature. © 1999 Kluwer Academic Publishers

## 1. Introduction

The mechanical properties of alumina ceramics can be improved by introducing mullite into the surface region. It has been shown that mullite can be formed on the surface of alumina by heating alumina in a bed of SiC powder [1] or by annealing a Si-deposited alumina in air [2]. In both cases, strength increases of >25% were reported. These increases were attributed to the presence of residual surface compressive stresses which were generated during cool-down after heat treatment due to the thermal expansion mismatch between alumina and mullite. However, these techniques yield only relatively low thicknesses of the compressive stress zones. Because strength-limiting flaws are typically in the order of 50 to 200  $\mu\text{m}$  [3], the flaws cannot be completely contained in the compression zone, which limits the strength improvement to moderate levels.

Recently, we have successfully fabricated three-layer RBAO-based composites with 40 vol % mullite in the outer layers [4]. Because the outer layers (that is, the compression zone) can be tailored to any desired thickness, such composites exhibit an excellent resistance to contact-induced damage. It was found that the initial strength of three-layered specimens with an outer layer thickness of 400  $\mu\text{m}$  can be retained even after indenting under a load of 300 N due to the existence of a residual compressive stress in the outer layers.

The magnitude of residual stresses can be determined by several techniques. In the present work, an indentation technique was chosen. The effects of the outer layer thickness on the distribution of residual stresses

in the layers of three-layer alumina composites were examined and are discussed in the present paper.

## 2. Experimental procedure

To obtain 40 vol % mullite in the outer layers and 17.5 vol % zirconia in the inner layer after reaction bonding, an initial powder consisting of 48.9 vol % Al (AS 081, <50  $\mu\text{m}$ , Eckart-Werke, Germany), 41.7 vol %  $\text{Al}_2\text{O}_3$  (Ceralox HPA-0.5, 0.5  $\mu\text{m}$ , Condea Chemie GmbH, Brunsbüttel, Germany), and 9.4 vol % SiC (F1000, 4.5  $\mu\text{m}$ , Norton AS, Lillesand, Norway) was selected for the outer layers, while a powder mixture of 50 vol % Al, 30 vol %  $\text{Al}_2\text{O}_3$  and 20 vol %  $\text{ZrO}_2$  (TZ-2Y, 24 nm, Tosoh Co., Tokyo, Japan) was used for the inner layer. The calculated final compositions are: 60 vol %  $\text{Al}_2\text{O}_3$ , 40 vol % mullite for the outer layers, and 82.5 vol %  $\text{Al}_2\text{O}_3$ , 17.5 vol %  $\text{ZrO}_2$  for the inner layer. Three-layer reaction bonded alumina composites with a total thickness of 5.2 mm and four different outer layer thicknesses (0.2, 0.4, 0.8 and 1.2 mm) were formed by first filling the outer layer powder into a rectangular die, then adding the inner layer powder followed by a second addition of the outer layer powder. The powders were then uniaxially pressed at 50 MPa and subsequently isostatically pressed at 300 MPa. Reaction bonding and sintering were performed in air with a sintering hold at 1550 °C for 1.5 h. Details of the fabrication process were described in a previous work [4]. In order to determine the residual stress distribution by the chosen indentation technique, the side-faces

of three-layer specimens were machined and polished to a  $1\ \mu\text{m}$  finish. Indentations were made in air using a Vickers diamond indenter at a load of 25 N with a holding time of about 25 s. Care was taken to orientate the indents so that one set of the radial cracks be parallel to the interfaces between layers. After unloading, the length of cracks perpendicular to the interfaces was immediately measured in order to minimize subcritical crack growth caused by atmospheric moisture.

### 3. Results and discussion

Fig. 1 shows a schematic of a three-layer specimen. An optical micrograph of such a material is given in Fig. 2. The sample is straight, bending does not occur because the layers are positioned symmetrically on two opposite sides. The outer layers of this sample are 0.4 mm thick on each side. Figs 3 and 4 show SEM micrographs of the layers and of the interface between them. There

is an approximately  $50\ \mu\text{m}$  thick porous zone at the interface.

The thermal expansion coefficients (TECs) of the inner layer ( $\alpha_i$ ) and the outer layers ( $\alpha_o$ ) were estimated to be  $8.52$  and  $6.9 \times 10^{-6}/^\circ\text{C}$  by using the simple mixture rule and taking the TECs of alumina, zirconia and mullite as  $8.1$ ,  $10.5$  and  $5.1 \times 10^{-6}/^\circ\text{C}$  [5]. During cooling down from sintering temperature, the inner layer would contract more than the outer layers if the layers were separated. However, in the case of a well-bonded interface between layers, the contraction of the inner layer is constrained by the outer layers. This leads to a tensile stress,  $\sigma_i$ , in the inner layer, and a compressive stress,  $\sigma_o$ , in the outer layers.

Based on the equilibrium of forces in the longitudinal direction, the residual stresses  $\sigma_i$  and  $\sigma_o$  are related by [6]

$$\sigma_i = -2 \cdot \frac{t_o}{t_i} \cdot \sigma_o \quad (1)$$

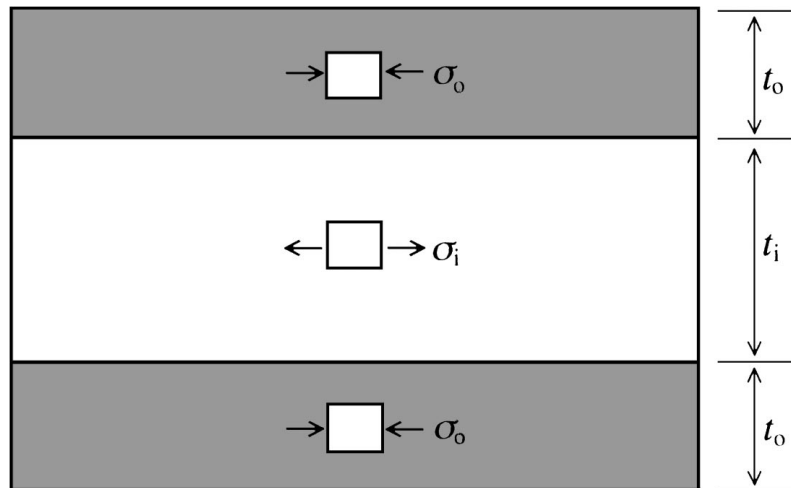


Figure 1 Schematic of an ideal three-layer specimen.

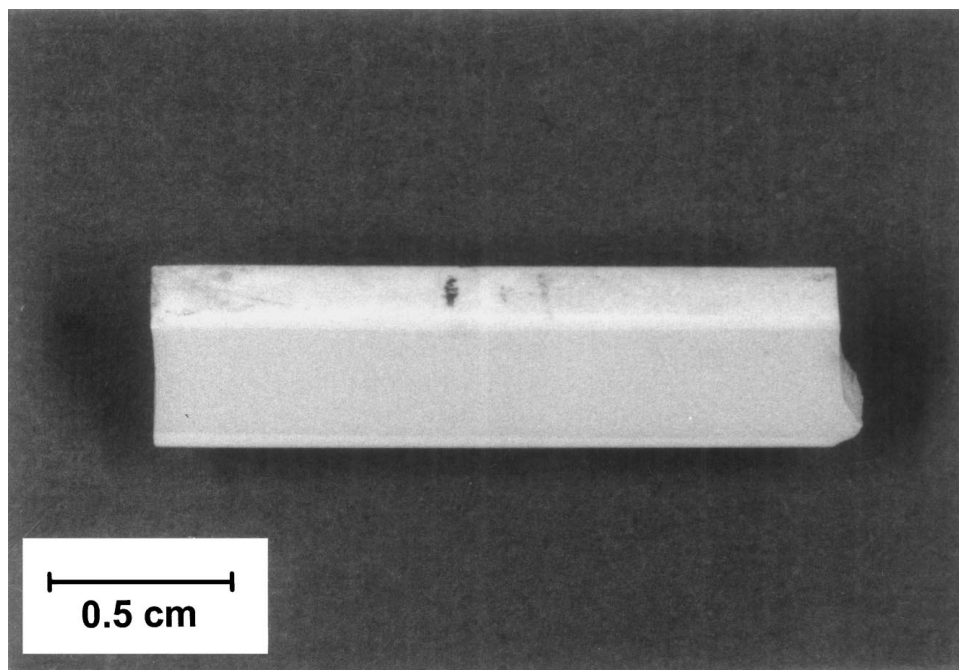


Figure 2 Optical micrograph of three-layer specimen.

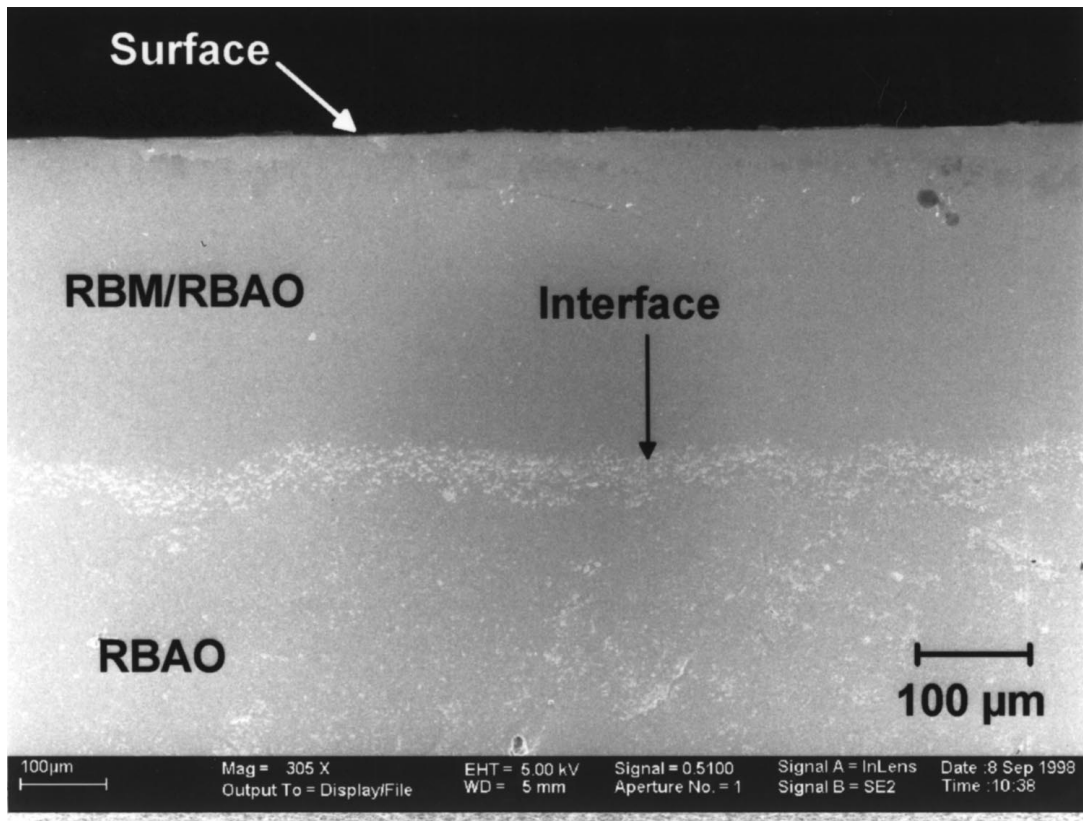


Figure 3 Scanning electron micrograph of three-layer specimen.

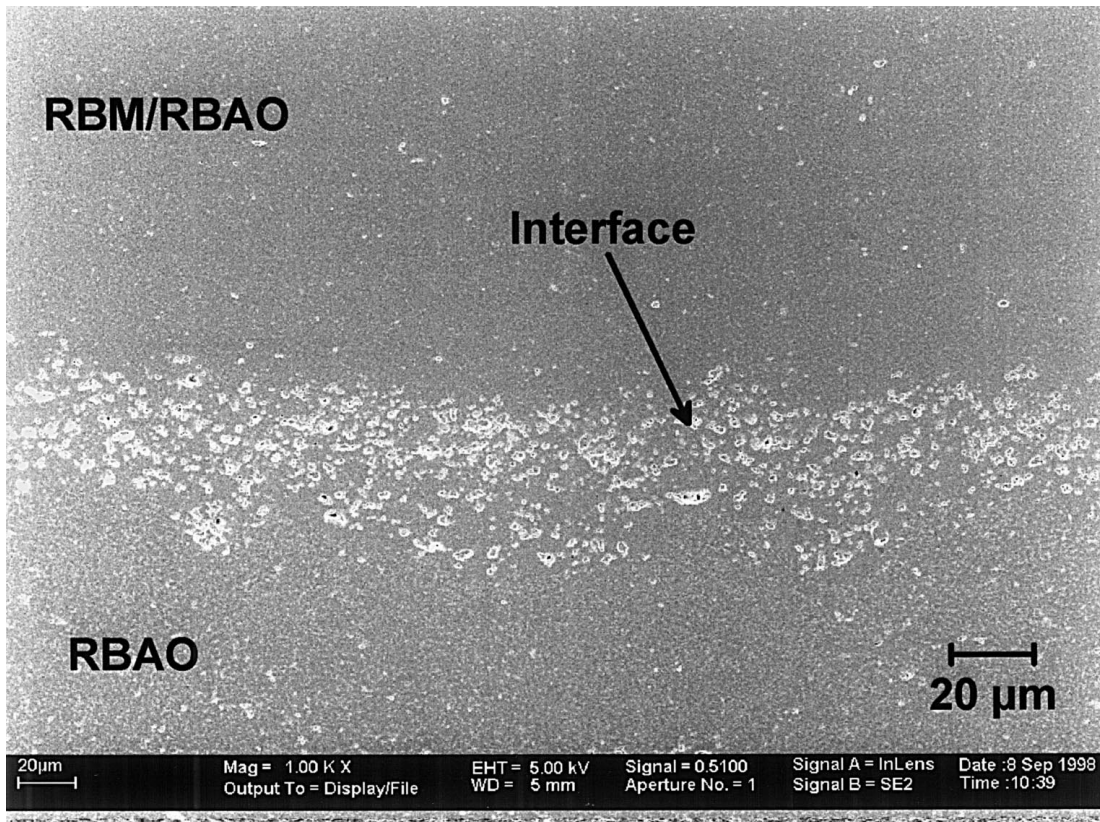


Figure 4 Scanning electron micrograph of three-layer specimen.

TABLE I Calculated residual stresses in the inner and outer layers for three-layer alumina composites with different outer-layer thicknesses

Outer-layer thickness <sup>a</sup> (mm)	Residual stress (MPa)	
	$\sigma_o$	$\sigma_i$
0.2	-583	48
0.4	-542	98
0.8	-456	203
1.2	-366	314

<sup>a</sup>The total thickness of all three-layer specimens is 5.2 mm.

where  $t_i$  and  $t_o$  are the thicknesses of the inner and outer layers, respectively. The magnitude of the residual compressive stress,  $\sigma_o$ , in the outer layers can be calculated from [7]

$$\sigma_o = (\alpha_o - \alpha_i) \cdot \Delta T \cdot \frac{E_o}{1 - \nu_o} \cdot \left[ 1 + 2 \cdot \frac{t_o}{t_i} \cdot \frac{E_o / (1 - \nu_o)}{E_i / (1 - \nu_i)} \right]^{-1} \quad (2)$$

where  $\Delta T$  is the effective temperature difference during cooling,  $E_o$  is the Young's modulus of the outer layers,  $E_i$  is Young's modulus of the inner layer,  $\nu_o$  is Poisson's ratio of the outer layers, and  $\nu_i$  is Poisson's ratio of the inner layer.

Table I gives the calculated values of the residual tensile and compressive stresses in the inner and outer layers for three-layer RBAO-composites with different outer layer thicknesses. In calculations,  $\Delta T$  was assumed to be 1000 °C, and the Young's moduli ( $E_i$ ,  $E_o$ ) and the Poisson's ratios ( $\nu_i$ ,  $\nu_o$ ) of the inner and outer layers were estimated by using the  $E$  and  $\nu$  data of alumina, zirconia and mullite [8]. Cooling down from sintering temperature was done relatively slowly at 10 °C/min, therefore no significant temperature gradient should exist between outer and inner layer. It can be seen in Table I that the residual compressive stress in the outer layers decreases, but the corresponding tensile stress in the inner layer increases with increasing outer layer thickness. At an outer layer thickness of 1.2 mm, a residual tensile stress of about 300 MPa is created in the inner layer. This can result in the extension of preexisting cracks and thereby cause a degradation of the mechanical properties. At an outer layer thickness of 0.4 mm, the residual tensile stress in the inner layer only amounts to  $\approx 100$  MPa, but the residual compressive stress in the outer layers reaches values up to  $\approx 550$  MPa. Judging from this, an excellent surface-flaw tolerance can be expected for such a composite. Measurements of the mechanical properties of layered specimens after indentation have shown strength values of 450 MPa in pressureless sintered samples and of 800 MPa in hot isostatically pressed samples even after indentation at a load of 300 N [4].

The magnitude of the residual stresses in the inner and outer layers can be determined by an indentation technique. When a stress-free ceramic is indented on the surface with a Vickers indenter, the radius,  $c_0$ , of the half-penny cracks is determined by the stress intensity factor,  $K_I$ , at the indentation crack tip [9]

$$K_I = \chi \cdot \frac{P}{c_0^{3/2}} \quad (3)$$

where  $P$  is the indentation load, and  $\chi$  is a dimensionless constant which depends on the modulus-to-hardness ratio. If the ceramic is in a residual tensile or compressive state, the crack-tip stress intensity factor,  $K_I$ , can be expressed as [10]

$$K_I = \chi \cdot \frac{P}{c^{3/2}} + \frac{2}{\sqrt{\pi}} \cdot \sigma_r \cdot \sqrt{c} \quad (4)$$

where  $c$  is the radius of the indentation cracks in the presence of a residual stress,  $\sigma_r$ .

For the case of very thin layers (layer thickness  $d \ll c$ ), the stress intensity factor can be expressed as [11]

$$K = \chi \frac{P}{c^{3/2}} + 2\psi \sigma_s d^{1/2} \quad (5)$$

where  $\psi$  is a crack geometry term. However, in our case, the layer thickness is greater than the crack length, therefore this term is only given for completeness here.

From Equations 3 and 4, it is easily derived that

$$\sigma_r = \frac{1}{2} \cdot K_I \cdot \sqrt{\frac{\pi}{c}} \cdot \left[ 1 - \left( \frac{c_0}{c} \right)^{3/2} \right] \quad (6)$$

Note that under a stable crack growth condition, the indentation stress intensity  $K_I$  amounts to the critical stress intensity, that is, the fracture toughness,  $K_{IC}$ , of the ceramic. Then, the residual stress,  $\sigma_r$ , can be obtained from Equation 6 based on accurate measurements of indentation crack lengths.

In the present work, monolithic reaction bonded alumina ceramics containing 17.5 vol% zirconia or 40 vol% mullite, respectively, were used as the 'unstressed' reference to determine the residual stresses in the three-layer composites. The monolithic materials have fracture toughness values of 4.65 and 3.0 MPa · m<sup>1/2</sup>, respectively. Figs 5–8 show the measured stress distribution over the total thickness of specimens with different layer thicknesses.

As can be seen, the outer layers are under a residual compression and the average stress values decrease with increasing outer layer thickness, while the residual stresses in the inner layer are tensile and the mean values

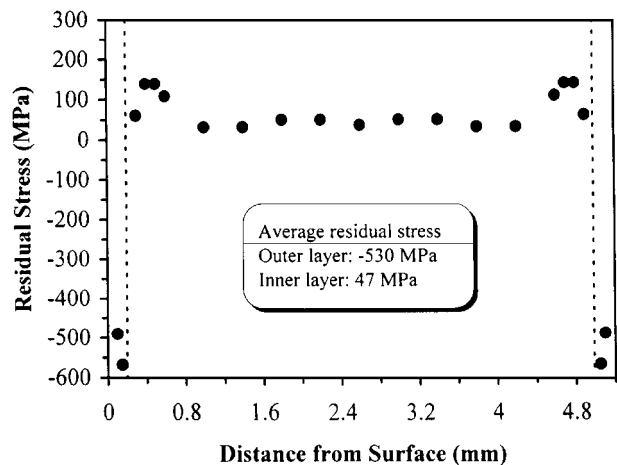


Figure 5 Residual stress distribution in the inner and outer layers of three-layer alumina composite with an outer-layer thicknesses of 0.2 mm.

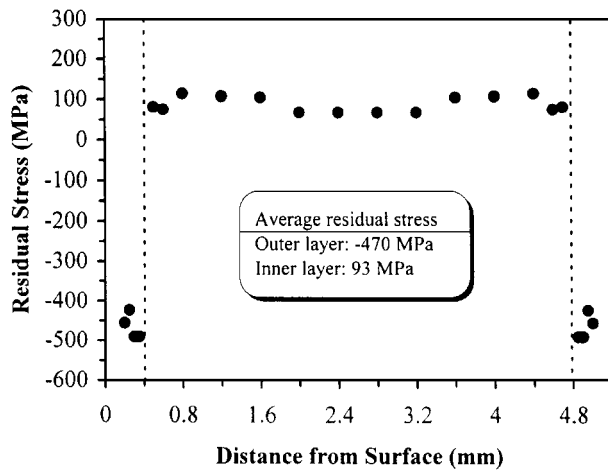


Figure 6 Residual stress distribution in the inner and outer layers of three-layer alumina composite with an outer-layer thicknesses of 0.4 mm.

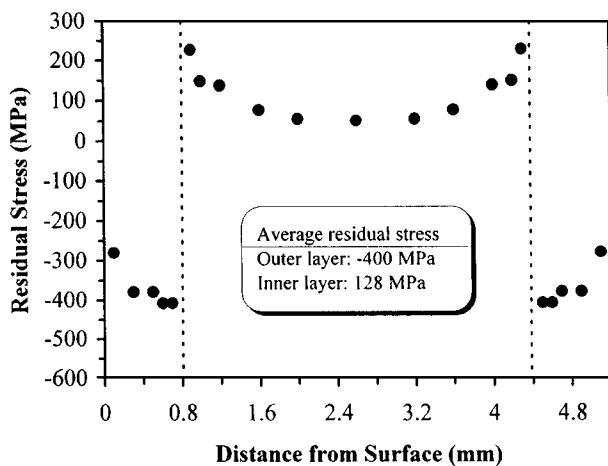


Figure 7 Residual stress distribution in the inner and outer layers of three-layer alumina composite with an outer-layer thicknesses of 0.8 mm.

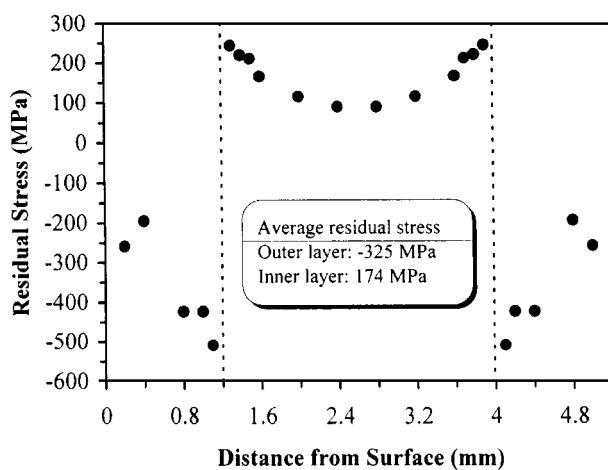


Figure 8 Residual stress distribution in the inner and outer layers of three-layer alumina composite with an outer-layer thicknesses of 1.2 mm.

of these stresses increase with increasing outer layer thickness. This is in good agreement with the theoretical calculations. However, the magnitude of the calculated residual stresses is only approximately achieved. The average measured values of the residual stresses in the inner and outer layers are lower than the calculated values in Table I. Furthermore, it is interesting to

TABLE II Comparison of calculated and measured residual stresses in the inner layer of three-layer alumina composites with different outer-layer thicknesses

Outer-layer thickness <sup>a</sup> (mm)	Residual stress (MPa)		
	Calculated	Measured	Deviation (%)
0.2	48	47	-2.1
0.4	98	93	-5.1
0.8	203	128	-36.9
1.2	314	174	-44.6

<sup>a</sup>The total thickness of all three-layer specimens is 5.2 mm.

note that the residual stress distribution is not uniform throughout each layer, but shows a considerable deviation in the vicinity of the interfaces. For specimens with outer layer thicknesses of 0.2 and 0.4 mm, the maximum residual compressive stress in the outer layers occurs near the interfaces, whereas the maximum tensile stress in the inner layer is found at a distance of approximately the outer layer thickness from the interfaces. This latter phenomenon is not yet understood, but it is consistent with the fact that the failure of three-layer specimens with an outer layer thickness of 0.4 mm originates from interior voids in the inner layer [4]. For specimens with outer layer thicknesses of 0.8 and 1.2 mm, the residual tensile and compressive stresses in the inner and outer layers reach a maximum near the interfaces, and decrease substantially with increasing distance from the interfaces. This indicates that there is a partial relaxation of residual stresses in the layers with increasing distance from the interfaces. This could occur through creep at high temperatures. On a macroscopic scale, three-layer specimens fabricated in this work were found to have concave side faces.

The data given in Table II show that the deviation between the calculated and the measured residual stresses in the inner layer increases with increasing outer layer thickness. At an outer layer thickness of 1.2 mm, the measured stress is 44.6% below the calculated value. Since the residual tensile stress in the inner layer increases with increasing outer layer thickness, a notable plastic deformation is expected for the inner layer at higher thicknesses of the outer layers. In this case, the residual stress will relax partially, thereby accounting for the difference between measured and calculated stress values.

#### 4. Conclusions

A simple indentation technique was used to determine the residual stresses in three-layer reaction bonded alumina composites containing 17.5 vol % zirconia in the inner layer and 40 vol % mullite in the outer layers. The results show that the outer layers are under a residual compressive stress while the inner layer is in a tensile stress state. The magnitudes of the residual stresses depend on the thickness of the outer layers. As the outer layer thickness increases, the residual compressive stress in the outer layers decreases, and the residual tensile stress in the inner layer increases. Compressive stresses of up to 550 MPa were measured in this study.

The measured residual stresses in the inner and outer layers are not uniform, but decrease with increasing distance from the interfaces. This is assumed to originate from creep during cooling down from the fabrication temperature.

### Acknowledgements

This work was supported by the Deutsche Forschungsgemeinschaft (DFG). Jihong She would like to express his gratitude towards the Deutscher Akademischer Austauschdienst (DAAD) for a K. C. Wong Research Fellowship.

### References

1. H. P. KIRCHNER, R. M. GRUVER and R. E. WALKER, *Trans. Brit. Ceram. Soc.* **70**(6) (1971) 215–219.
2. S. NODA, H. DOI, T. HIOKI, J. I. KAWAMOTO and O. KAMIGAITO, *J. Amer. Ceram. Soc.* **69**(9) (1986) C-210–C-212.
3. A. V. VIRKAR, J. L. HUANG and R. A. CUTLER, *ibid.* **70**(3) (1987) 164–170.
4. J. H. SHE, S. SCHEPPOKAT, R. JANSSEN and N. CLAUSSEN, *ibid.* **81**(5) (1998) 1374–1376.
5. R. KAMO and W. BRYZIK, *Ceram. Eng. Sci. Proc.* **5**(5/6) (1984) 312–338.
6. R. LAKSHMINARAYANAN and D. K. SHETTY, *J. Amer. Ceram. Soc.* **79**(1) (1996) 79–87.
7. O. SBAIZERO and E. LUCCHINI, *J. Eur. Ceram. Soc.* **16**(8) (1996) 813–818.
8. W. J. LACKEY, D. P. STINTO, G. A. CERNY, A. C. SCHAFFHAUSER and L. L. FEHRENBACHER, *Adv. Ceram. Mater.* **2**(1) (1987) 24–30.
9. G. R. ANSTIS, P. CHANTIKUL, B. R. LAWN and D. B. MARSHALL, *J. Amer. Ceram. Soc.* **64**(9) (1981) 533–538.
10. D. B. MARSHALL and B. R. LAWN, *J. Mater. Sci.* **14**(8) (1979) 2001–2012.
11. B. R. LAWN and E. R. FULLER JR, *ibid.* **19** (1984) 4061–4067.

*Received 21 November 1997  
and accepted 15 October 1998*